
Article:
Hoffmann, T., Sharon, O., Wittmann, J. et al. (2018) NaV1.7 and pain: contribution of peripheral nerves. Pain, 159 (3). pp. 496-506. ISSN: 0304-3959

https://doi.org/10.1097/j.pain.0000000000001119

$Na_V1.7$ and pain: contribution of peripheral nerves

Running title: Sensory phenotyping $Na_V1.7$ knock-outs

Tal Hoffmann[1*], Ohad Sharon[1*], Jürgen Wittmann[2], Richard W. Carr[3], Alina Vyshnevska[3], Roberto De Col[1], Mohammed A. Nassar[4], Peter W. Reeh[1] and Christian Weidner[1,5]

[1] Institute for Physiology and Pathophysiology, University of Erlangen-Nuremberg
Universitaetsstrasse 17, 91054 Erlangen, Germany

[2] Division of Molecular Immunology, Department of Internal Medicine III, Nikolaus-Fiebiger Center for Molecular Medicine, University of Erlangen-Nuremberg
Glückstrasse 6, D-91054 Erlangen, Germany

[3] Department of Anaesthesiology and Operative Intensive Care, University of Heidelberg, 68167 Mannheim, Germany

[4] Biomedical Science, University of Sheffield, S10 2TN, United Kingdom

[5]Health and Food safety Authority, Eggenreuther Weg 43, 91058 Erlangen, Germany

* Both authors contributed equally

Author to whom correspondence should be addressed:

Tali Hoffmann

Phone: +49 – 9131 - 8526730

Fax: +49 – 9131 - 8522497

Email: tal.hoffmann@fau.de

Abbreviation list:

Action potential (AP); Activity-dependent slowing (ADS); Afterhyperpolarization (AHP); A-fiber compound action potential (A-CAP); C-fiber compound action potentials (C-CAP); high-threshold mechanosensitive C-fiber (C-HTM); Congenital indifference to pain (CIP); Calcitonin gene-related peptide (CGRP); low-threshold mechanosensitive C-fiber (C-LTM); mechano-cold sensitive C-fiber (CMC); mechano-heat sensitive C-fiber (CMH); mechano-heat-cold sensitive C-fiber (CMHC); Dorsal root ganglion (DRG); Knock – out mice (KO); Receptive field (RF); Synthetic interstitial fluid (SIF); Tetrodotoxin (TTX); Tetrodotoxin resistant (TTXr); Tetrodotoxin sensitive (TTXs); Transient receptor potential vanilloid 1 (TRPV1); Voltage-gated sodium channels (VGSC);.

Key words: voltage-gated sodium channels, unmyelinated fibers, CGRP release, compound action potential, plantar test, von Frey test

INTRODUCTION

The TTX-sensitive sodium voltage-gated channel $Na_v1.7$, encoded by the SCN9A gene has been in the center of latest research concerning pain mechanisms and the development of new analgesics. Human gain-of-function mutations lead to erythromelalgia [35;60], small fiber neuropathy [18;23;23;42] and paroxysmal extreme pain disorder [17;29;61], in all of which pain perception is excessive. Increased channel expression and activity have also been reported in peripheral neuropathic and diabetic rat models [19;28;33;49;52;59;62]. In contrast, human loss-of-function mutations cause congenital indifference to pain (CIP) and anosmia [1;13;22]. These symptoms are also present in mutant mice, both conditional and global knock-outs, presenting with subnormal pain behavior in several pain models and behavioral signs of anosmia [11;21;31;40;49;58].

In the olfactory system $Na_v1.7$ is expressed in the soma, axon and synaptic bouton of olfactory sensory neurons [2;58]. Likewise, in the nociceptive system it is present in small dorsal root ganglion neurons (DRG), their unmyelinated axons as well as cutaneous terminals [7;41;46], and it is largely absent in the CNS [54], suggesting that initiation, conduction and first synaptic transmission of action potentials might critically depend on $Na_v1.7$ and explain the phenotype of knock-out animals and missense mutations in humans. However the fact that the histamine-evoked axon reflex is unaltered in CIP patients [22], while itch perception is absent [21], suggests that spike initiation and peripheral nociceptive conduction are at least partly functional in spite of the absence of $Na_v1.7$. Likewise, it has recently been shown in a CIP patient and $Na_v1.7$ conditional knock-out animals that naloxone can partially restore pain [38]. This means that at least part of the peripheral input must reach the presynapse, but due to synaptic inhibition induced by an upregulated opiodergic system in $Na_v1.7$ deficient animals/humans is not transmitted further centrally. However, for the olfactory system of

63 $Na_v1.7$-deficient animals transmission failure has been shown, action potentials properly
64 generated in sensory neurons do not initiate synaptic signaling [58].

65 These studies indicate that peripheral somatic nerves may still generate action potentials and
66 propagate, at least part of them, centrally in the absence of $Na_v1.7$. In the light of the
67 biophysical properties of $Na_v1.7$, its absence would be expected to have an influence on
68 initiated conduction of action potentials in peripheral nerves. Its relatively hyperpolarized
69 activation and inactivation voltage in comparison to $Na_v1.8$ [3;50] and its rapid
70 activation/inactivation kinetics [30] make it suited as an amplifier of subthreshold
71 depolarizations, setting the spike threshold. Furthermore, its slow repriming [24], its
72 prominently slow closed-state inactivation and recovery [14] and the ability to generate
73 resurgent currents [18] are indicative of determining discharge patterns and neural
74 accommodation.

75 So far, studies on pain pathways in $Na_v1.7$ global [21] or conditional knock-out mice
76 [36;37;40] focus on pain behavior or DRG discharge or currents. Here we compare generation
77 and conduction of action potentials and their accommodation in the peripheral sensory
78 endings and nerves of DRG-selective (Advillin/Cre) SCN9A knock-out and wild-type mice.
79 Apart from general physiological interest, for development of drugs targeting $Na_v1.7$ it is
80 essential to know whether a compound should engage the neuron before or behind the blood-
81 brain barrier.

82

83

84

MATERIALS AND METHODS

Chemicals and solutions

Synthetic interstitial fluid (SIF, [10]) solution used for single-fiber recordings, compound action potential experiments and CGRP release measurements consisted (in mM) of: 107.8 NaCl, 26.2 $NaCO_3$, 9.64 Na-gluconate, 7.6 sucrose, 5.05 glucose, 3.48 KCl, 1.67 NaH_2PO_4, 1.53 $CaCl_2$ and 0.69 $MgSO_4$, continuously gassed with carbogen (95% oxygen and 5% carbon dioxide) equilibrating the solution at pH 7.4. Addition of potassium for 60mM depolarizing KCl solution was compensated by subtraction of an equimolar NaCl concentration.

Animals

The Advillin-Cre transgenic mice, were a generous gift from J. N. Wood [37]. Floxed $SCN9A^{loxP/loxP}$ mice were kindly supplied by T. Leinders-Zufall [58]. The $Na_V1.7$ gene was selectively deleted in sensory neurons expressing Advillin, by crossing Advillin-Cre with $SCN9A^{loxP/loxP}$ mice [37]. Genomic DNA from the tails of KO mice was genotyped using the polymerase chain reaction (PCR). The following primers were used (Invitrogen) for Advillin-Cre genotyping: primer1 (Adv forward) - CCCTGTTCACTGTGAGTAGG, primer2 (Adv WT-reverse) – AGTATCTGGTAGGTGCTTCCAG and primer3 (Adv-Cre reverse) - GCGATCCCTGAACATGTCCATC. Following a 3 min period at 96°C, DNA samples were denaturated (96°C 30sec), annealed (63°C, 30sec) and extended (72°C, 1min) for 30 cycles with a subsequent 10 min period at 72°C. The wildtype band from Primers 1+2 was 480 bp long and mutant allele from Primers 1+3 was 180 bp long. The Primers used for loxP genotyping: primer4 (SCN9A forward) - CAGAGATTTCTGCATTAGAATTTGTTC, Primer5 (SCN9A WT/floxed reverse) – AGTCTTTGTGGCACACGTTACCTC and Primer6 (SCN9A KO reverse) - GTTCCTCTCTTTGAATGCTGGGCA. Following a 2 min period at

94°C, DNA samples were amplified (94°C 30sec), annealed (60°C, 30sec) and extended (72°C, 2min) for 34 cycles. Wildtype band from primers 4+5 was 317 bp long, loxP allele from primers 4+5 was 461 bp long and a $Na_V1.7$ KO allele was indicated by a 395 bp long band from Primers 4+6. Both Advillin-Cre and $SCN9A^{loxp/loxp}$ mice were continuously crossed with C57BL6 to congenity so C57BL/6 mice were used as control animals [58]. Inbred C57BL/6 and $Na_V1.7^{Adv}$ conditional KO mice of both sexes and ranging in weight between 20-25g were housed in group cages in a temperature-controlled environment with a 12h light-dark cycle and were supplied with food and water *ad libitum*. Animals were killed in a rising CO_2 atmosphere in accord with German and European laws.

Transcriptional regulation

Total RNA was extracted from homogenized dorsal root ganglia (10-20 ganglia per mouse, 3 mice from each genotype) with the RNeasy Mini kit and treated with DNaseI (QIAGEN, Hilden, Germany). First-strand cDNA was synthesized from 150 ng oligo(dT)-primed RNA with the RevertAid Reverse Transcriptase kit from Thermo Fisher Scientific. For quantitative real-time RT-PCR (qRT-PCR) analysis, cDNA reactions were mixed with 2x Absolute QPCR Mix, SYBR Green, Rox Mix (Thermo Fisher Scientific), the appropriate primers (from Thermo Fisher Scientific) and filled with water to 20 µl. $Na_V1.7$ Primer sequences are listed above under "Animal" section, otherwise, the following Primers were used (all in 5' → 3' direction): ACTB qRT-PCR forward – CGGTTCCGATGCCCTGAGGCTCTT, ACTB qRT-PCR reverse – CGTCACACTTCATGATGGAATTGA. Expected product: 100 bp. SCN8A qRT-PCR forward - CGTACTATTTGACGCAGAAAACTT. SCN8A qRT-PCR reverse – TCATGCTGAAGACTGAATGTATCA. Expected product: 153 bp. SCN9A qRT-PCR forward – GCCTTGTTTCGGCTAATGAC, SCN9A qRT-PCR reverse – TCCCAGAAATATCACCACGAC. Expected product: 111 bp. SCN10A qRT-PCR forward –

GTGTGCATGACCCGAACTGAT, SCN10A qRT-PCR reverse – CAAAACCCTCTTGCCAGTATCT. Expected product: 101 bp. SCN11A qRT-PCR forward – CCCCTGACCTTATAGCGAAGC, SCN11A qRT-PCR reverse – CTCTTGGCGCTGAAGCGATA. Expected product: 112 bp. Primers were initially tested at concentrations of 100, 300 and 900 nM and finally used at 300 nM. qPCRs including no-template and reverse transcriptase-minus controls were performed in triplicates in an Applied Biosystems 7300 Real-Time PCR System (Applied Biosystems, Darmstadt, Germany) with 15 minutes as initial stage at 95°C to activate the DNA polymerase, followed by 40 PCR cycles of 95°C for 15 sec and 60°C for 1 minute. Dissociation curves were generated by heating to 95°C for 15 sec, 60°C for 30 sec and 95°C for 15 sec. PCR products were additionally separated on agarose gels and visualized by ethidium bromide staining. Standardization was performed by quantification of the beta Actin gene as an endogenous control and the ΔΔCt method. A cut-off of above twofold increase/decrease was set as a criterion for changes in gene expression. Statistical analysis was performed on at least three independent experiments (i.e., mice) and results are shown as fold increase in $Na_V1.7$ KO mice vs. C57BL6 controls.

Behavioral tests

All animal experiments were approved by the responsible appropriate Animal Protection Authority (Regierung von Unterfranken, Würzburg, Germany). Paw withdrawal latency measurements were performed on both male and female 8-10 weeks old mice. All mice were tested in a "blind" manner, with the person performing the measurements unaware of the mouse genotype. After acclimatization to the testing environment (a few hours exposure to the experimental environment in the two consecutive days prior to the experiment), mice were subjected to repeated plantar mechanical and heat stimulation. Mechanical threshold of the

paw was determined using a dynamic plantar aesthesiometer (Ugo Basile, Gemonio, Italy). A movable unit supplied with a von Frey filament (0.5mm diameter) applied linearly increasing forces onto the plantar side of the hindpaw until withdrawal, at which point the threshold force was recorded. Measurements were done on alternating feet (at least 6 times per mouse), with at least 3 min pause between each stimulus, and results from each mouse were averaged. For thermal stimulation, an infrared light beam was focused to the plantar side of the hindpaw (Ugo Basile, Gemonio, Italy) through a grid floor on which the mice were allowed to walk unrestricted. The beam was automatically switched off upon withdrawal of the paw, recording the latency. Both left and right paw were measured alternately (at least 8 measurements per mouse) with minimum 3 minutes between stimulations. Two radiant heat stimuli of different intensity (7 and 9 in arbitrary units) were alternately applied and latencies for each intensity were averaged. The total number of sensory stimuli per animal (mechanical + thermal) was between 14 and 20.

Single-fiber electrophysiology

Single-fiber recordings from cutaneous C fibers of the saphenous nerve were obtained using the isolated skin-nerve preparation as described previously [26;43].

Mechanosensitive receptive fields were mapped using a blunt glass rod. Once a distinct receptive field was identified, electrostimulation was applied to the RF through a metal microelectrode to determine the fiber's conduction velocity. Values of conduction velocity were used for classification with a cut-off criterion of <1.4 m/s for unmyelinated (C) fibers [6]. $Na_V1.7$ is primarily expressed in small DRGs and unmyelinated nerve fibers [7;46] thus, electrophysiological recordings in this study were focused solely on unmyelinated C fibers. Lack of initial spontaneous activity was a prerequisite for further testing of all units. A

179 marking technique was applied, in which latency shifts are provoked through simultaneous
180 application of mechanical and electrical stimuli to the RF [48], ensuring recording from a
181 distinct single-fiber. To assess sensory properties, the mechanical threshold of fibers was
182 characterized using calibrated von Frey (polyamide) bristles ranging in force from 1-128 mN
183 in a geometric scale and equipped with varnished tips (Ø 0.8mm). Subsequent to
184 characterisation, a metal ring (9 mm diameter) was placed encircling the RF. Vaseline was
185 applied to the base of the ring to improve fluid isolation. The fluid volume within the ring was
186 replaced by ice-cold buffer for noxious cold stimulation, or heated by a thermode coupled to a
187 custom-made Peltier device for noxious heat stimulation (20 s ramp of 32 ° - 46 °C). Each
188 stimulus was followed by a resting period of several minutes prior to onset of the following
189 stimulus to minimize the risk of sensitizing effects between modalities. Fibers were
190 considered cold/heat responsive if they produced at least 2 spikes concurrent to stimulation
191 onset. Heat threshold was defined as the temperature at which the second spike of the heat
192 response occurred.

193 The electrical excitability of the cutaneous nerve endings was determined as the voltage
194 threshold for eliciting an action potential. Rectangular constant voltage stimuli of variable
195 width (in ms: 0.02, 0.2, 2, 20, 200) were applied to the most mechanosensitive spot within the
196 receptive field. Activity-dependent slowing (ADS) of conduction velocity was measured
197 during an electrical stimulation protocol consisting of a 3 min pause, 6 min 0.25 Hz, 3 min 2
198 Hz, 6 min 0.25 Hz [20]. Changes in conduction velocity are expressed as percentage of initial
199 values (at stimulation onset) of the individual nerve. Maximal slowing is calculated for the
200 last 30 sec of the 2 Hz stimulation. In addition, a recovery cycle protocol at 0.2ms and
201 supramaximal strength was performed, [9;57]. In a continuous stimulation frequency of 0.5
202 Hz single conditioning pre-pulses at different inter-stimulus intervals (6-500 ms) were

interposed and the latency shift of the conditioned action potential as compared to its conditioning predecessor was analyzed. Finally, some of the fibers were electrically challenged at the RF with ongoing paired electrical pulses (20 ms intrastimulus intervals) at 2 Hz [20;56] and 2-3 fold individual threshold voltage (increased if necessary to compensate for a possible drift of electrical threshold). This provides the time required to provoke conduction block as an index of conduction reliability. Conduction block was defined as the condition when the paired pulses ceased to yield two discernible spikes.

Compound action potential recordings

Compound action potential (CAP) signals were recorded extracellularly from isolated segments of mouse saphenous nerve. The saphenous nerves from C57BL/6 and $Na_V1.7^{Adv}$ knock-out mice were dissected bilaterally from their point of leaving the inguinal region to approximately 5mm below the knee. Nerves were desheathed to remove the epi- and perineurium and placed in a recording chamber between two suction electrodes. The bath was perfused continuously with SIF, bubbled continuously with carbogen (95% O_2 : 5%CO_2) to a pH of 7.4. Experiments were performed in room temperature as at this temperature the superimpost action potential was still above detection level in all nerves. For electrical stimulation and recording the cut ends of the nerve were pulled through a silicon membrane, creating an optimal seal of the recording and stimulating neuronal sites. The chamber is a modification of the previously published one [12]. Silver wire electrode served as the cathode and anode for stimulation for one suction electrode and for a differential recording at the other. CAP responses were evoked using constant current stimulation (A395, WPI, Sarasota, USA) of fixed duration (1 ms) For the determination of amplitude and conduction velocity (i.e conduction latency over the fixed recording distance of 5 mm between electrodes) the C-fibre CAP response to supra-maximal electrical stimulation was assessed. To elucidate CAP

changes in response to a repetitive stimulation challenge, a stimulus protocol was used comprising 3 min pause followed by 6 min at 0.25 Hz, 3 min at 2.5 Hz, 6 min at 0.25 Hz (1/4 s). Changes in conduction latency and CAP amplitude during this protocol are expressed as percentage change of their initial value at stimulation onset, i.e. relative to the first value after the 3minute pause.

CGRP release

Flaps of the hairy skin from the lower leg and foot were excised and wrapped around acrylic glass rods (6mm diameter) with the corium side exposed, as previously described [47]. Samples were placed in carbogen gassed SIF (equilibrating the solution at pH 7.4) and positioned in a shaking bath set to 32°C for a washout period of 30min. Skin flaps were then consecutively passed through a set of 4 glass tubes containing 800µl SIF. Each incubation step lasted 5min. The first 2 incubation steps were to determine basal CGRP release at 32°C. The third incubation step assessed stimulus-induced CGRP release and the reaction tubes contained either SIF at 47°C or SIF with 60mM KCl. The fourth incubation step assessed recovery of the response in SIF solution at 32°C. CGRP levels were determined using commercial enzyme immunoassays (EIAs; Bertin Pharma, Montigny, France), as previously described [5]. Samples were photometrically analyzed using a microplate reader (Opsys MR^{TM}, Dynex Technologies, Chantilly, Virginia, USA).

Statistics

Statistical analysis was performed using the Statistica software package 7.0 (Statsoft). For multiple groups comparison one-way analysis of variance (one-way ANOVA) was used. Other statistical tests used are denoted in the text. $P < 0.05$ was considered statistically significant (depicted as * in the figs). All data is presented as mean ± SEM.

RESULTS

Behavioural tests in naive animals

Behavioral tests in animals represent the integrative performance of both central and peripheral nervous systems. We tested the mechanical and heat sensitivity of $Na_V1.7^{Adv}$ conditional KO vs. congenic control mice. From their general appearance, control animals could not be differentiated from KOs, which were as heavy, big, groomed and vigilant as controls. By a blinded examiner, two heat stimulus intensities were tested in each group, both revealing a significantly longer withdrawal latency in $Na_V1.7^{Adv}$ KOs (Fig. 1A): 27.4 $\pm$ 3.3 sec for the lower stimulus intensity (7 arbitrary units) and 25.5 $\pm$ 3 sec for the higher intensity (9 arbitrary units), versus 14 $\pm$ 2.6 sec and 12.6 $\pm$ 2.8 sec, respectively, in controls ($p<0.05$ U-Test). Though less substantial, the mechanical threshold (dynamic von Frey) was also significantly elevated in KOs (Fig. 1B): 4.2 $\pm$ 0.7 mN versus 3.1 $\pm$ 0.6 mN in controls ($p<0.05$ U-Test).

Recordings from unmyelinated cutaneous single-fibers

The lack of $Na_v1.7$ in peripheral sensory neurons resulted in reduced behavioural noxious heat and mechanical responsiveness of mice. We therefore tested whether this deficiency would be recapitulated in the properties of the cutaneous nerve endings. 60 mechanosensitive cutaneous C-units from controls and 30 from $Na_V1.7^{Adv}$ KOs were recorded. The fiber population from controls comprised (Fig. 2A): 45 mechano-heat sensitive C-fibers (CMH; 75%), 10 C high threshold mechanosensitive fibers (C-HTM; 17%), 2 low-threshold mechanosensitive C-fibers (C-LTM; 3%), 2 mechano-cold sensitive C-fibers (CMC; 3%) and 1 mechano-heat-cold C-fiber (CMHC; 2%). The fiber population in $Nav1.7^{Adv}$ KO was significantly different from that of controls, with mechano-heat sensitive fibers no longer being the most abundant (χ^2 (df

= 4, n= 90) = 15, p< 0.001): 10 CMH fibers (33%), 13 C-HTM fibers (43%), 4 CMC (13%), 2 C-LTM (7%) and 1 CMHC (3%). The sensory capacities (mechanical and thermal) of the fiber populations from both genotypes were compared. The mechanosensitivity of the KO units did not significantly differ from that of controls (Fig. 2B-C). The 10 $Na_V1.7^{Adv}$ KO C-fibers that were heat sensitive surprisingly seemed more responsive to heat than the control units (with higher discharge rate during stimulation, though not significant, Fig. 2D) and a lower mean heat threshold in comparison to controls (37.9 $\pm$ 1.5 °C and 40.3 $\pm$ 0.4 °C, respectively, Fig. 2E, p=0.059, U-Test).

We next examined the conductive properties of the single units. The mean conduction velocity of KO fibers was significantly lower than that of controls by about 20%, while the variance was about the same (Fig 3A-B, 0.4 $\pm$ 0.04 m/s vs. 0.5 $\pm$ 0.02 m/s, respectively ($p<0.05$ U-Test). The single-fiber recordings from $Na_V1.7$ KO mice have not shown reduced sensitivities to the diverse modalities of mechanical and heat stimulation. A possible explanation for that would be that the voltage threshold for triggering propagated action potentials in the skin nerve endings is about the same in KOs and WTs. We therefore assessed the electrical excitability, placing an electrode (cathode) in the receptive field at the spot of highest mechanosensitivity. In addition to varying the stimulus voltage, we also varied the stimulus duration in order to gain information about a potential kinetic difference between KO and WT nerve terminals. However, the resulting strength-duration curves did not significantly differ between the genotypes (Fig. 3C, left graph, multiple T-tests with Bonferroni correction). Also the chronaxy did not appear different between KO and WT. This became evident when the parabolic curve was linearized by plotting the product of threshold voltage and stimulus duration (an analogue to threshold charge transfer) over stimulus duration in a linear coordinate system (Fig. 3C right graph). In this representation the chronaxy

297 corresponds to the abscissa intercept, which is obviously the same in both genotypes, whereas
298 the slightly different slopes of the (regression) lines correspond to the non-significant
299 difference of the rheobases. This means that the kinetic requirements (utilization times) of the
300 electrical stimulus to trigger an action potential are not different between $Na_V1.7$-/- and WT.
301 In other words, $Na_V1.7$ is not required as an action potential generator in those C-fibers that
302 retained mechanosensitivity and electrical excitablity in the KOs.

303 The recovery cycle experiment (Fig. 3D) with electrical double pulses at varying inter-
304 stimulus intervals (ISI) studies the impact of a preceding action potential on the conduction
305 velocity (latency) of the subsequent, second, spike. Apart from the prolonged latency (slower
306 conduction velocity) in KOs vs. WTs, visible at longer ISI (> 100 ms), the exponential
307 increase of the latency with shorter ISIs (< 100 ms) in the KO fibers is striking and obviously
308 different from the moderate increase in WT fibers. These changes are attributed to long
309 lasting afterpotentials, most probably of hyperpolarizing direction. Thus, $Na_V1.7$ seems to
310 stabilize the conduction velocity at shorter spikes intervals (higher discharge rates).

311 This role of $Na_V1.7$ in stabilizing conduction velocity lead us to examine the activity-
312 dependent slowing of conduction velocity (ADS) upon prolonged low frequency (e.g. 2 Hz)
313 stimulation. This phenomenon is due to progressive slow inactivation of the voltage-gated
314 sodium channels and to accumulation of sodium ions in the thin nerve fibers [15;53]. During a
315 control period of 6 min at 0.25 Hz the fibers became slightly slower in conduction, showing
316 no difference between both genotypes (Fig 4A). During the more frequent electrical
317 stimulation at 2 Hz for 3 min, the ADS became progressively prominent in the WTs, but the
318 KO fibers soon lagged behind and finally reached clearly less maximal ADS than the WT
319 units (Fig. 4B: 35.5 $\pm$ 6.2% vs. 57.4 $\pm$ 4.7%, respectively, $p<0.05$, U-Test). During the
320 subsequent recovery period of 6 min at 0.25 Hz both latencies returned towards their original

values. Progressive ADS of single units often leads to conduction failures, in which condition fibers do not reliably respond to each electrical stimulus with a propagated action potential. Our stimulation test was a 4 min period of 2 Hz double-pulse (ISI 20 ms) stimulation. In accord with the finding of less ADS, the KO fibers were much less prone to block in comparison to controls, more reliably responding to the second of the paired stimuli (Fig. 4C, block of 6/13 units as opposed to 12/13, respectively).

In conclusion and comparison to WT fibers, the mechanosensitive cutaneous C-fibers that we could identify in $Na_V1.7^{Adv}$ KO mice, exhibited (1) a significantly lower prevalence of responsiveness to moderate noxious heat, although (2) the rarer heat responses seemed to show exceptionally high mean discharge rates and low heat thresholds; (3) mechanosensitivity was about normal. In biophysical respects, (4) conduction velocity was 20% slower and (5) became progressively slower in response to the second of two electrical stimuli applied at short interval (< 100 ms); (6) electrical excitability, rheobase and chronaxy, were about normal. Upon prolonged electrical stimulation at 2 Hz, (7) activity-dependent slowing of nerve fiber conduction was markedly less expressed and (8) more rarely led to conduction failure of the KO single-fibers. Above all, it seems that a subpopulation of moderately heat responsive polymodal nociceptors is, at least functionally missing in $Na_V1.7^{Adv}$ mice, while the retained and detectable C-fibers in these mice exhibit anomalous biophysical properties tha do not indicate any susceptibility to failure of action potential generation or conduction.

Stimulus-induced cutaneous CGRP release

The single-fiber recordings suggested the absence of a subpopulation of heat sensitive nociceptors in $Na_V1.7^{Adv}$ KO mice. A way to test the overall heat responsiveness of a skin flap is to measure stimulated CGRP release which can serve as an index for the activation of, at least, the peptidergic neurons [26]. However, hindpaw skin flaps of $Na_V1.7^{Adv}$ KO and control

mice revealed no significant difference in CGRP release evoked by heating to 45°C or, for control, by depolarisation with 60mM KCl (Fig. 5). This CGRP release depends on calcium influx through heat-activated ion channels or voltage-gated calcium channels, respectively, but not on action potential generating sodium channels [51]. Thus, the results exclude the absence of a peptidergic subpopulation of fibers, e.g. for possible developmental reasons in the transgenic mice, but they do not exclude the functional inability of these fibers to generate propagated action potentials.

Compound action potential recordings

The single-fiber recordings from the saphenous innervation territory suggested both the functional absence of a whole subpopulation of conducting C-fibers and altered conduction properties of the retained C-fibers as a result of the conditional deletion of $Na_V1.7$ in the DRGs. Both consequences should show up in whole saphenous nerve recordings of the compound action potentials. Indeed, the A-fiber CAP amplitudes were about the same in KOs and WTs, but the C-CAPs of the KO mice were by two thirds smaller and half as fast in conduction velocity than in the WTs (Fig. 6A-C). These deficits can hardly be due to dispersion (in time) of the electrically evoked action potentials, as the single-fiber spikes showed about the same amplitudes and even slightly less scattering of the reduced conduction velocities in KOs as compared to WTs (see above). Also the finding of less ADS in KOs than WTs was fully recapitulated in the C-CAP recordings (Fig. 6D).

Transcriptional regulation

It has previously been shown that in $Na_V1.8$ KO mice there is transcriptional upregulation of $Na_V1.7$ mRNA [4], also of relevance for neuronal excitability in whole animals [34;63]. To make sure our results do not stem from similar transcriptional upregulation we have screened

368 KOs for expression of specific sodium channels. Quantitative PCR results from DRGs
369 demonstrate that the conditional KOs had no significant change in gene expression of $Na_v1.6$,
370 $Na_v1.8$ and $Na_v1.9$ in comparison to control mice (Fig 7).

371

372

DISCUSSION

Na_V 1.7 human mutations cause either extremely painful diseases or indifference to pain without further neurological deficits except for anosmia. Several studies have used knock-out models of Na_V 1.7 to elucidate the phenotype related to the gene deletion with behavioural testings or recordings from second order lamina V neurons in the spinal dorsal horn of primary neurons [21;37;40]. In contrast, we focused on the hypothesis of a subthreshold amplifying function of Nav1.7. We found no difference in the mechanical thresholds between KOs and WTs and heat sensitive fibers the KOs did not present reduced, but rather insignificantly enhanced heat responsiveness. This was most likely due to the fact that more than half of the "normal" polymodal nociceptors with moderate heat responses (< 25 spikes in a 20 s ramp from 32°-46°C) were missing in the KO skin. In their place the fraction of high-threshold mechanosensitive and mechano-cold sensitive C-fibers was relatively enlarged from 20% in WT to 56% in the KOs.

A central question is whether these typical polymodal C-fibers are physically absent in Na_V1.7Adv KOs, or just unable to generate/ propagate action potentials along their axons? At least one essential function; neuropeptide (CGRP) release from cutaneous sensory axons and terminals was largely unaffected in the KOs. This important function requires the presence of peptidergic nerve fibers connected by axonal transport to their DRG cell bodies, but it does not require action potential discharge, just depolarization and calcium influx are sufficient [51]. The axon reflex erythema upon histamine injection is reported to be functional in human CIP mutants [22]. This suggests that action potentials are generated and (antidromically) conducted through wide branching arborisation of the CGRP-expressing nerve fibers. It does however not mean that these action potentials are propagated up the peripheral nerve.

Our previous studies with pharmacological elimination of Na_V 1.7 by TTX indicate that actually almost all cutaneous C-fibers are more or less affected by the toxin, at least at higher temperatures [63]. This raises the question whether the subpopulation of single-fibers compensating the lack of NaV1.7 by other channels such as NaV 1.8 or 1.9 in our present study show biophysical symptoms resulting from the Na_V1.7 deletion. An interplay of the two major players Na_V1.7 and Na_V1.8 has been made responsible for electrogenesis in DRG neurons [44]. While Na_V1.7 opens in the subthreshold range and amplifies slow small depolarisations (often together with Na_V1.9) Na_V1.8 takes over at more depolarised membrane potentials to finally carry most the APs sodium influx ([25], for review see [55]). Rapid repriming and relative resistance to inactivation make Na_V1.8 also responsible for conduction safety [27]. However this interplay depends on cell type. Rush and colleagues have shown, that an erythermalgia gain of function mutation of Na_V1.7 (L858H) may result in hyperexcitability of DRG neurons but hypoexcitability of sympathetic neurons [45]. Likewise neurons – or even sections of one neuron (soma, axon, terminal) - with different expression patterns or availability patterns (i.e. inactivity patterns at various resting membrane potentials) of sodium channels (Na_V1.8 in the above example) might modulate this interplay.

Changes of electrogenesis in the axon is expected to have an influence on conduction velocity. In modelling studies conduction velocity (of myelinated fibres) has been predicted to be mainly influenced by sodium channel kinetics i.e. composition of kinetically different subtypes is more important than overall channel density [39]. Indeed, we found conduction velocity of Na_V1.7 deficient axons to be significantly lower by 20% than in WT fibers. Using the same methods, we could not see altered conduction velocity in Na_V1.8 [27] or Na_V1.9 [26] knock out animals. However unmyelinated axons lacking Na_V1.6 [8] also slow down conduction of compound action potentials by ~30%. A lack of the persistent current of Na_V1.6

might have hyperpolarised these axons and thereby slowed down conduction. Also our results suggest hyperpolarisation of $Na_V1.7$ deficient terminals. The recovery cycle experiments revealed a pronounced sub-normality at double-pulse intervals shorter than 100 ms in the KOs, much less in the WTs. This is reminiscent of the exceptionally long after-hyperpolarizations, up to 100 ms, that DRG neurons with nociceptive C-fibers show [32].

Indeed, the conduction velocity of the units was significantly lower by 20% than in WT fibers. The recovery cycle experiments revealed a pronounced sub-normality at double-pulse intervals shorter than 100 ms in the KOs, much less in the WTs. This is reminiscent of the exceptionally long after-hyperpolarizations, up to 100 ms, that DRG neurons with nociceptive C-fibers show [32]. If this finding also applies to nerve endings, $Na_V1.7$ could rapidly recover from fast voltage-dependent inactivation during the AHP and quickly respond to the subsequent electrical stimulus, due to its relatively hyperpolarized activation range. If, however, $Na_V1.8$ has to initiate the action potential, as in the KOs, it will take longer to reach its more depolarized activation voltage range starting from a still hyperpolarized membrane potential and, accordingly, the conduction velocity will drop. The underlying difference in voltage-dependent activation between $Na_V1.7$ and $Na_V1.8$ is well established in DRG neurons [16]. However, it does not seem to apply to the unmyelinated nerve endings in the skin, as the parameters of electrical excitability, rheobase and chronaxy, were not significantly different between $Na_V1.7$Adv KOs and WTs. This should not be due to an insufficient power of resolution of the extracellular electrostimulation technique, because the expectable reduction of excitability in global $Na_V1.9$ KOs could recently be demonstrated using the same threshold tracking technique [26]. Thus, the reason for the discrepancy between DRG cell bodies and their cutaneous terminals remains unclear but may relate to the fundamental difference in membrane surface – to – volume ratio.

444 The experiments on activity-dependent slowing of the conduction velocity refer to a different
445 time scale than the recovery cycle trials, the interstimulus interval was 500 ms and the
446 challenge of the C-fibers by continuous electrical stimulation lasted for 3 min. During this
447 period the ADS in WTs finally reached a plateau which was significantly lower in the KOs.
448 Two parallel mechanisms seem to account for the ADS phenomenon, an accumulation of
449 slow voltage-dependent inactivation of the sodium channels and an accumulation of sodium
450 ions inside the thin axons which reduces their inward driving force [15;53]. We tend to
451 assume that the absence of the $Na_V1.7$-carried sodium current, reducing the accumulation, is a
452 reason for less ADS in the KOs. Both mechanisms can obviously lead to conduction failures,
453 in particular at branch points. This affected every single one of the WT fibers but only half of
454 the KO units during a 4 min challenge with 2 Hz double pulses. Again, we assume that less
455 sodium accumulation is responsible for this increased safety factor of conduction in the KOs.

456 We found many functional nociceptive C-fibers in the saphenous of $Na_V1.7^{Adv}$ KOs but also
457 an indication that one heat sensitive subpopulation of units was reduced, either physically
458 absent or unable to conduct action potentials. Our compound action potential recordings
459 cannot decide between these alternatives, but they suggest that a subpopulation of C-fibers is
460 not conducting at normal peripheral skin temperature (32°C). A principal problem with CAPs
461 is that their amplitude can shrink either by enhanced dispersion of the individual fiber
462 conduction velocities or by reduced size or number of the superimposed action potentials.
463 However, the single-fiber recordings did not reveal a greater scattering of the spike latencies
464 in the KOs and the spike amplitudes appeared normal with respect to the signal-to-noise ratio.
465 The conduction velocities were slower than in WTs, but this was also reflected by the C-CAP
466 which was equally slower in conduction in the KOs. Thus, most probably, it is the number of

467 superimposed C-fiber APs that is reduced in the KOs, in contrast to the A-fibers, for which A-
468 CAPs were not different between KO and WTs.

469 In synopsis of our results, we were surprised to find plenty of largely normal C-fiber
470 nociceptors in a transgenic mouse model of the human congenital indifference to pain (CIP)
471 syndrome. There is still a long distance to cover up from the peripheral saphenous nerve to the
472 spinal dorsal horn synapses, and the T-junction in the DRG as well as many branch points in
473 the dorsal horn have to be overcome by the action potentials. It seems that a subpopulation of
474 peripheral C-fibers is able to generate but not to properly propagate action potentials as in
475 primary olfactory neurons of conditional $Na_V1.7$ KO mice that are able to generate action
476 potentials but not to initiate synaptic signalling in the olfactory bulb [58]. Even though
477 upregulation of opiodergic inhibition has recently been made responsible for reduced
478 nociceptive input in CIP [38], this cannot be expected to be the only reason as it cannot
479 explain anosmia. The subpopulation of peripheral C-fibres shown in this study to depend on
480 $Na_V1.7$ for action potential propagation would also be expected to reduce nociceptive input by
481 drugs targeting $Na_V1.7$ without crossing the blood-brain barrier.

482

483 **ACKNOWLEDGMENTS**

484 The authors would like to thank Birgit Vogler and Annette Kuhn for excellent technical
485 assistance.

486 This article was funded by the Deutsche Forschungsgemeinschaft, grant RE 704/2-1 (to PWR
487 and CW) and the Bavarian equal opportunities sponsorship – Förderung von Frauen in
488 Forschung und Lehre (FFL, to TH).

Conflict of interest: The authors declare no conflict of interest.

FIGURES/LEGENDS

Fig. 1: Behavioural tests in conditional $Na_v1.7^{Adv}$ KO vs. congenic WT control mice. A. Blind testing of radiant heat-induced hindpaw withdrawal (Hargreaves´ test) using two stimulus intensities (7 and 9, arbitrary units). B. Dynamic von Frey testing of mechanical hindpaw withdrawal thresholds. Asterisks indicate $p<0.05$ using U-test.

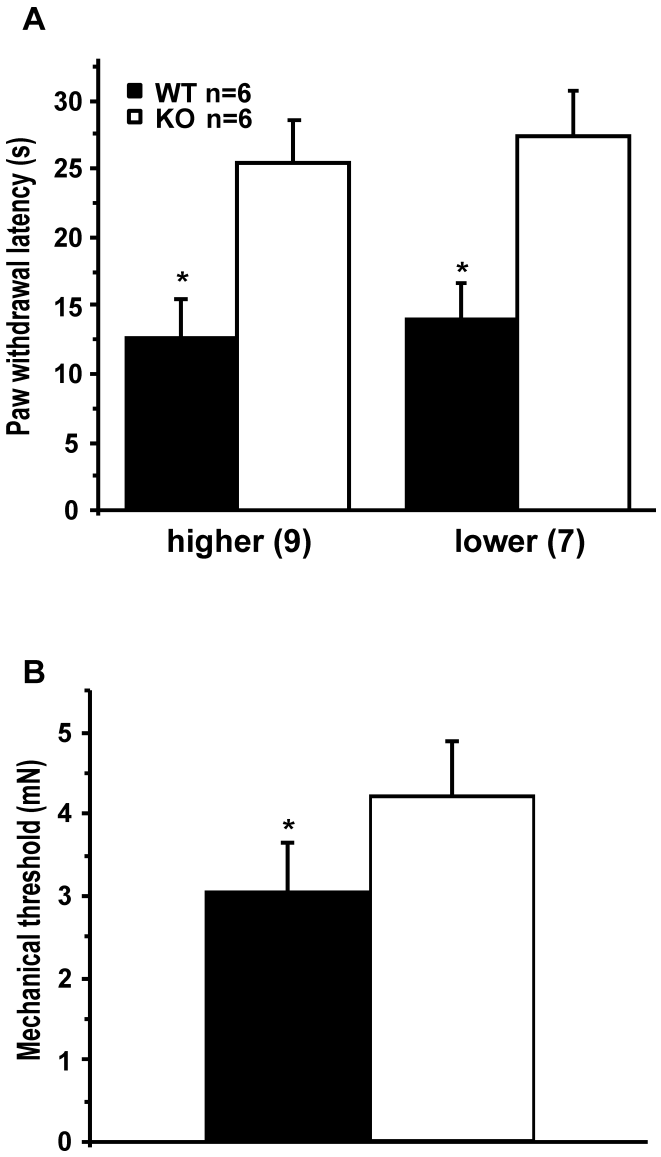

Fig. 2: Cutaneous C-fiber populations and sensory properties in $Na_v1.7^{Adv}$ KOs vs. WTs. A. Sensory categorization of mechanosensitive unmyelinated single-fibers *in vitro* reveals differential prevalence between the genotypes, in particular with respect to heat sensitivity (χ^2 (df = 4, n= 90) = 15, p< 0.001). **B.** Distribution of dynamic von Frey thresholds in KOs and WTs over a geometric force scale. **C.** Boxplot of the mechanical thresholds. **D.** Averaged discharge rates per second in response to a 20 s radiant heat ramp (grey background); large variability in KO fibers due to small sample size. **E.** Mean heat thresholds of the units (temperature at second spike, U-test).

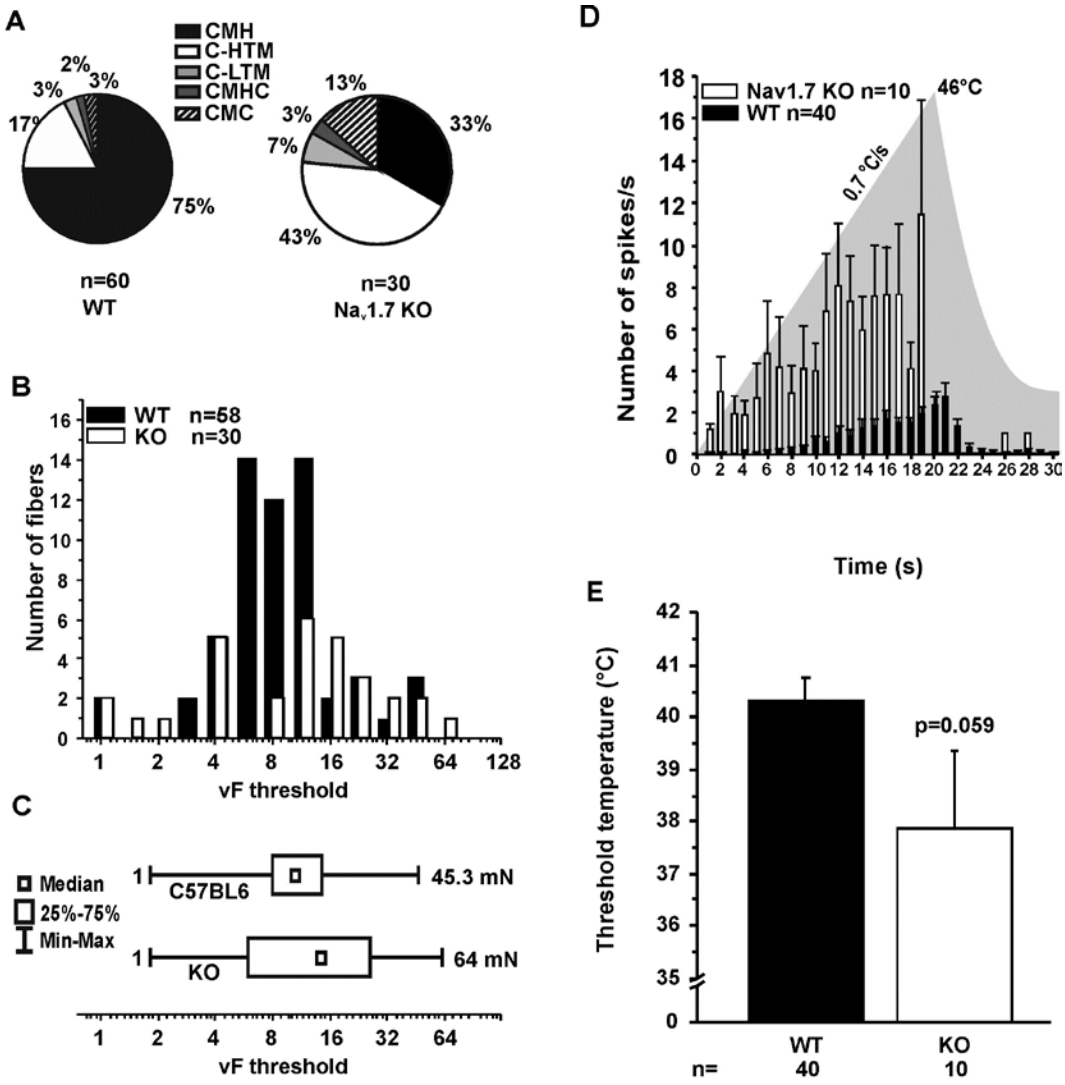

Fig. 3: Conductive properties of C-fibers in KOs and WTs. A. Distribution of conduction velocities over the distance from cutaneous receptive field to recording electrode. **B.** Modified boxplot showing mean instead of median; asterisk indicates $p<0.05$, U-test. **C.** Strength-duration curves determined by threshold tracking with electrode in the receptive field (left graph). Right graph: The parabolic curves in the left graph are linearized by calculating an analog to threshold charge transfer (V · ms), showing the slopes (i.e. rheobases) of the regression lines and identical abscissa intercepts (i.e. chronaxies). **D.** Electrical double pulses at varying ISI reveal differential retardation of the second spike, in particular at short intervals ($p < 0.05$, multiple T-tests with Bonferroni correction).

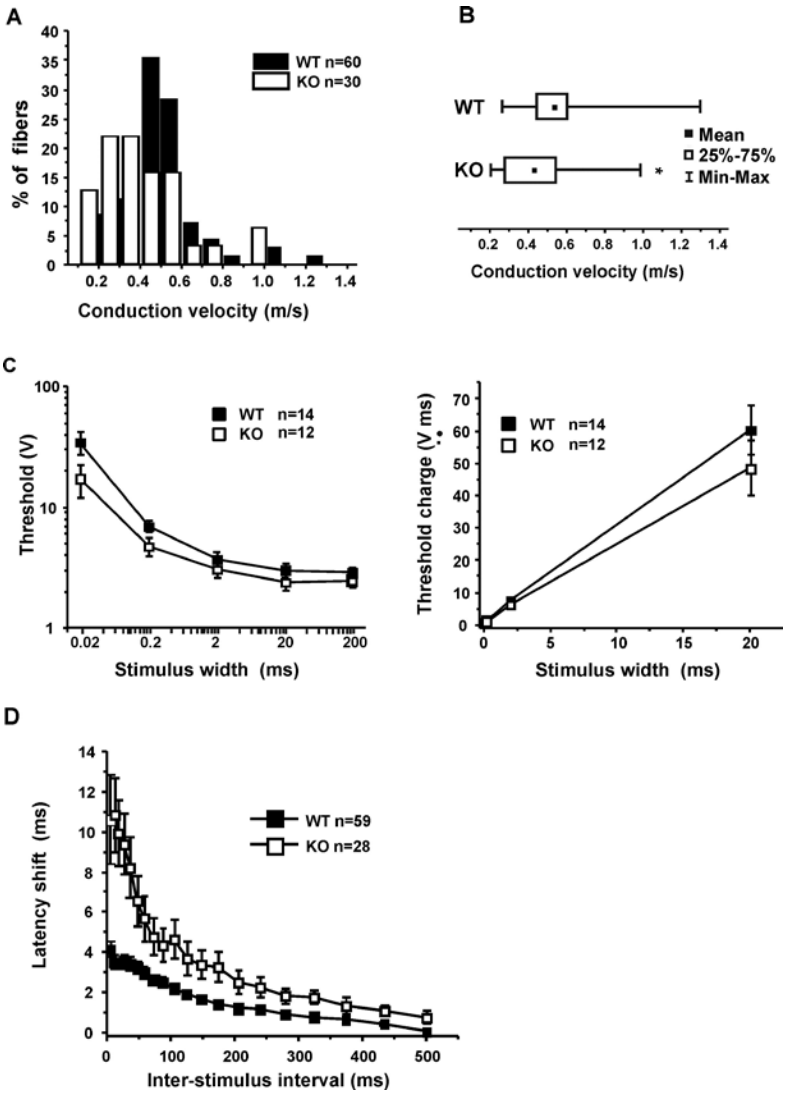

Fig. 4: Activity-dependent slowing and propagation safety of C-fibers in KOs and WTs. **A.** Differential ADS development over time in percent of initial latency. **B.** Maximal ADS, mean (± SEM) during the last 30 s of the 2 Hz stimulation period, the asterisk indicates $p<0.05$, U-test. **C.** Conduction failures during 4 minutes of electrical double pulse (20 ms ISI) stimulation at 2 Hz. The decreasing number of fibers reliably conducting over time is depicted.

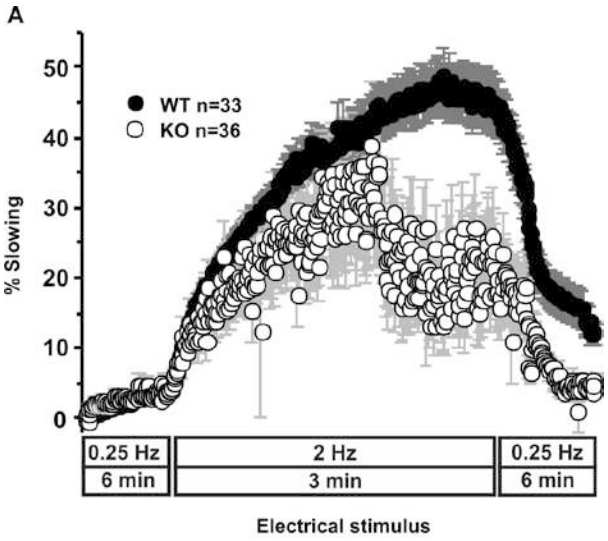
A
WT n=33
KO n=36
% Slowing
0.25 Hz
6 min
2 Hz
3 min
0.25 Hz
6 min
Electrical stimulus

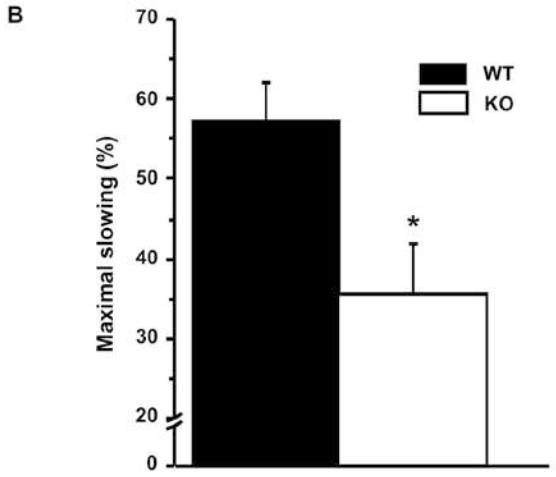
B
WT
KO
Maximal slowing (%)
*

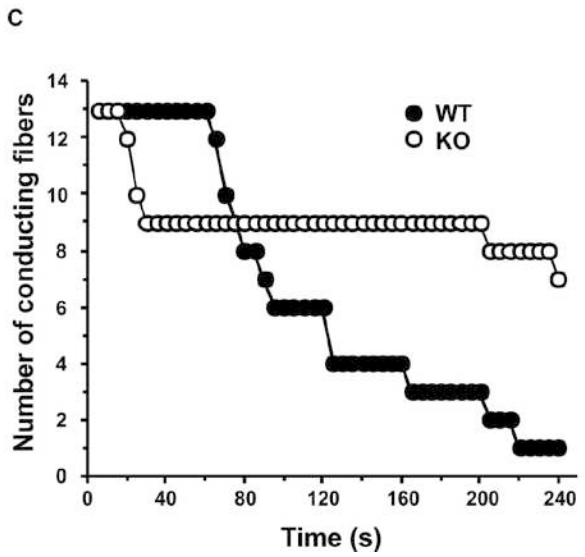
C
WT
KO
Number of conducting fibers
Time (s)

521

522

Fig. 5: Stimulated CGRP release from isolated skin. A. Response to 45°C heat stimulation. **B.** Response to unspecific depolarisation with 60 mM external KCl.

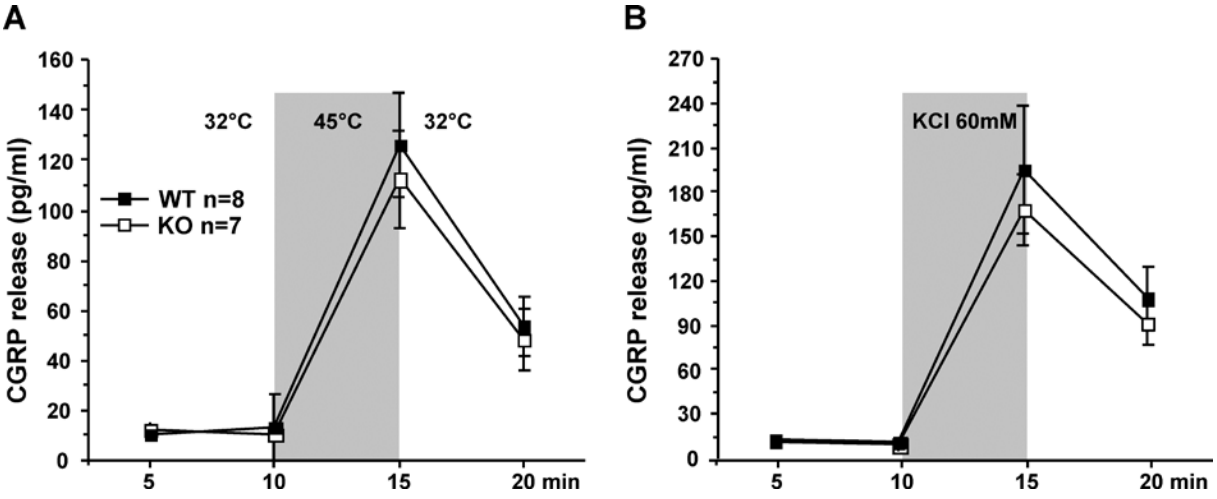

Fig. 6: Compound action potentials of isolated saphenous nerves of KOs and WTs. A. Single nerve examples showing fused electrical artefact and A-fiber CAPs as well as C-CAPs of differential latency and amplitude at 32°C. **B.** Conduction velocity of C-Caps, the asterisk indicates $p<0.05$, U-test. **C.** Peak-to-peak amplitudes of C- and A-CAPs, the asterisk indicates $p<0.05$, U-test. **D.** Development of ADS of the C-CAPs.

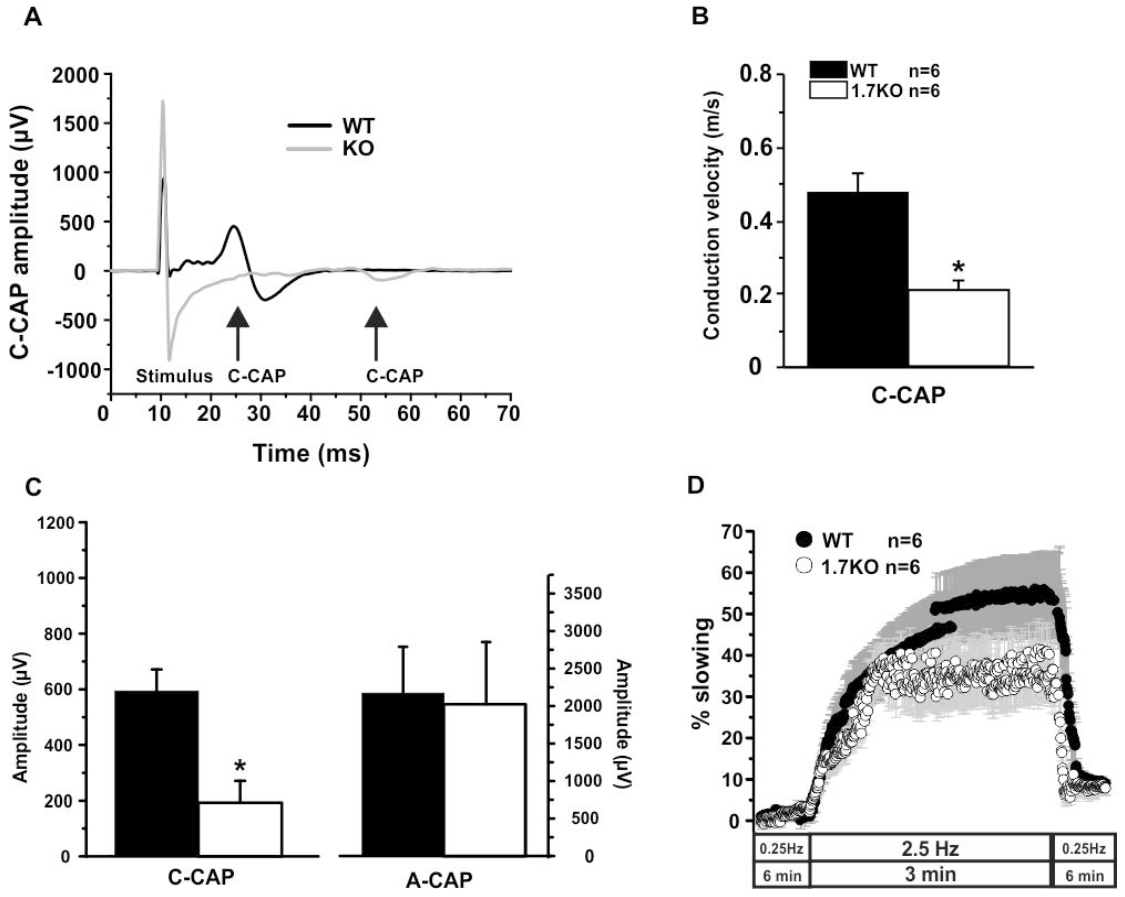

534

535 **Fig. 7: Gene expression in DRGs from $Na_V1.7$ KO mice.** Results are shown as fold change

536 of gene expression in KOs vs. control mice.

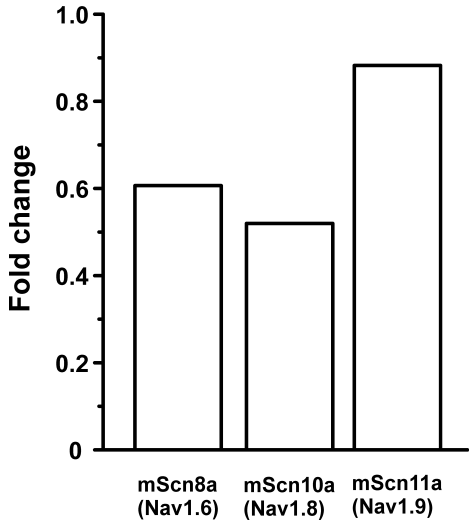

537

538

539 **Reference List**

540

541 **[1] Ahmad S, Dahllund L, Eriksson AB, Hellgren D, Karlsson U, Lund PE, Meijer**
542 **IA, Meury L, Mills T, Moody A, Morinville A, Morten J, O'donnell D,**
543 **Raynoschek C, Salter H, Rouleau GA, Krupp JJ. A stop codon mutation in**
544 **SCN9A causes lack of pain sensation. Hum Mol Genet 2007;16:2114-2121.**

545 **[2] Ahn HS, Black JA, Zhao P, Tyrrell L, Waxman SG, Dib-Hajj SD. Nav1.7 is the**
546 **predominant sodium channel in rodent olfactory sensory neurons. Mol Pain**
547 **2011;7:32.**

548 **[3] Akopian AN, Sivilotti L, Wood JN. A tetrodotoxin-resistant voltage-gated sodium**
549 **channel expressed by sensory neurons. Nature 1996;379:257-262.**

550 **[4] Akopian AN, Souslova V, England S, Okuse K, Ogata N, Ure J, Smith A, Kerr**
551 **BJ, McMahon SB, Boyce S, Hill R, Stanfa LC, Dickenson AH, Wood JN. The**
552 **tetrodotoxin-resistant sodium channel SNS has a specialized function in pain**
553 **pathways. Nat Neurosci 1999;2:541-548.**

554 **[5] Averbeck B, Reeh PW, Michaelis M. Modulation of CGRP and PGE2 release**
555 **from isolated rat skin by alpha-adrenoceptors and kappa-opioid-receptors.**
556 **Neuroreport 2001;12:2097-2100.**

557 **[6] Bessou P, Perl ER. Response of cutaneous sensory units with unmyelinated fibers**
558 **to noxious stimuli. J Neurophysiol 1969;32:1025-1043.**

559 **[7] Black JA, Frezel N, Dib-Hajj SD, Waxman SG. Expression of Nav1.7 in DRG**
560 **neurons extends from peripheral terminals in the skin to central preterminal**
561 **branches and terminals in the dorsal horn. Mol Pain 2012;8:82.**

562 **[8] Black JA, Renganathan M, Waxman SG. Sodium channel Na(v)1.6 is expressed**
563 **along nonmyelinated axons and it contributes to conduction. Brain Res Mol**
564 **Brain Res 2002;105:19-28.**

565 **[9] Bostock H, Campero M, Serra J, Ochoa J. Velocity recovery cycles of C fibres**
566 **innervating human skin. J Physiol 2003;553:649-663.**

567 **[10] Bretag AH. Synthetic interstitial fluid for isolated mammalian tissue. Life Sci**
568 **1969;8:319-329.**

569 **[11] Cai W, Cao J, Ren X, Qiao L, Chen X, Li M, Zang W. shRNA mediated**
570 **knockdown of Nav1.7 in rat dorsal root ganglion attenuates pain following burn**
571 **injury. BMC Anesthesiol 2016;16:59.**

572 **[12] Carr RW, Sittl R, Fleckenstein J, Grafe P. GABA increases electrical excitability**
573 **in a subset of human unmyelinated peripheral axons. PLoS One 2010;5:e8780.**

574 **[13] Cox JJ, Reimann F, Nicholas AK, Thornton G, Roberts E, Springell K, Karbani**
575 **G, Jafri H, Mannan J, Raashid Y, Al-Gazali L, Hamamy H, Valente EM,**
576 **Gorman S, Williams R, McHale DP, Wood JN, Gribble FM, Woods CG. An**
577 **SCN9A channelopathy causes congenital inability to experience pain. Nature**
578 **2006;444:894-898.**

579 **[14] Cummins TR, Howe JR, Waxman SG. Slow closed-state inactivation: a novel**
580 **mechanism underlying ramp currents in cells expressing the hNE/PN1 sodium**
581 **channel. J Neurosci 1998;18:9607-9619.**

582 **[15] De Col R, Messlinger K, Carr RW. Conduction velocity is regulated by sodium**
583 **channel inactivation in unmyelinated axons innervating the rat cranial meninges.**
584 **J Physiol 2008;586:1089-1103.**

585 **[16] Dib-Hajj SD, Cummins TR, Black JA, Waxman SG. Sodium channels in normal**
586 **and pathological pain. Annu Rev Neurosci 2010;33:325-347.**

587 **[17] Dib-Hajj SD, Estacion M, Jarecki BW, Tyrrell L, Fischer TZ, Lawden M,**
588 **Cummins TR, Waxman SG. Paroxysmal extreme pain disorder M1627K**
589 **mutation in human Nav1.7 renders DRG neurons hyperexcitable. Mol Pain**
590 **2008;4:37.**

591 **[18] Faber CG, Hoeijmakers JG, Ahn HS, Cheng X, Han C, Choi JS, Estacion M,**
592 **Lauria G, Vanhoutte EK, Gerrits MM, Dib-Hajj S, Drenth JP, Waxman SG,**
593 **Merkies IS. Gain of function Nanu1.7 mutations in idiopathic small fiber**
594 **neuropathy. Ann Neurol 2012;71:26-39.**

595 **[19] Fukuoka T, Miyoshi K, Noguchi K. De novo expression of Nav1.7 in injured**
596 **putative proprioceptive afferents: Multiple tetrodotoxin-sensitive sodium**
597 **channels are retained in the rat dorsal root after spinal nerve ligation.**
598 **Neuroscience 2015;284:693-706.**

599 **[20] George A, Serra J, Navarro X, Bostock H. Velocity recovery cycles of single C**
600 **fibres innervating rat skin. J Physiol 2007;578:213-232.**

[21] Gingras J, Smith S, Matson DJ, Johnson D, Nye K, Couture L, Feric E, Yin R, Moyer BD, Peterson ML, Rottman JB, Beiler RJ, Malmberg AB, McDonough SI. Global Nav1.7 knockout mice recapitulate the phenotype of human congenital indifference to pain. PLoS One 2014;9:e105895.

[22] Goldberg YP, MacFarlane J, MacDonald ML, Thompson J, Dube MP, Mattice M, Fraser R, Young C, Hossain S, Pape T, Payne B, Radomski C, Donaldson G, Ives E, Cox J, Younghusband HB, Green R, Duff A, Boltshauser E, Grinspan GA, Dimon JH, Sibley BG, Andria G, Toscano E, Kerdraon J, Bowsher D, Pimstone SN, Samuels ME, Sherrington R, Hayden MR. Loss-of-function mutations in the Nav1.7 gene underlie congenital indifference to pain in multiple human populations. Clin Genet 2007;71:311-319.

[23] Han C, Hoeijmakers JG, Ahn HS, Zhao P, Shah P, Lauria G, Gerrits MM, te Morsche RH, Dib-Hajj SD, Drenth JP, Faber CG, Merkies IS, Waxman SG. Nav1.7-related small fiber neuropathy: impaired slow-inactivation and DRG neuron hyperexcitability. Neurology 2012;78:1635-1643.

[24] Herzog RI, Cummins TR, Ghassemi F, Dib-Hajj SD, Waxman SG. Distinct repriming and closed-state inactivation kinetics of Nav1.6 and Nav1.7 sodium channels in mouse spinal sensory neurons. J Physiol 2003;551:741-750.

[25] Herzog RI, Cummins TR, Waxman SG. Persistent TTX-resistant Na+ current affects resting potential and response to depolarization in simulated spinal sensory neurons. J Neurophysiol 2001;86:1351-1364.

622 **[26] Hoffmann T, Kistner K, Carr RW, Nassar MA, Reeh PW, Weidner C. Reduced**
623 **excitability and impaired nociception in peripheral unmyelinated fibers from**
624 **Nav1.9-null mice. Pain 2017;158:58-67.**

625 **[27] Hoffmann T, Kistner K, Nassar M, Reeh PW, Weidner C. Use dependence of**
626 **peripheral nociceptive conduction in the absence of TTXr sodium channel**
627 **subtypes. J Physiol 2016.**

628 **[28] Hu J, Song ZY, Zhang HH, Qin X, Hu S, Jiang X, Xu GY. Colonic**
629 **Hypersensitivity and Sensitization of Voltage-gated Sodium Channels in Primary**
630 **Sensory Neurons in Rats with Diabetes. J Neurogastroenterol Motil 2016;22:129-**
631 **140.**

632 **[29] Jarecki BW, Sheets PL, Jackson JO, Cummins TR. Paroxysmal extreme pain**
633 **disorder mutations within the D3/S4-S5 linker of Nav1.7 cause moderate**
634 **destabilization of fast inactivation. J Physiol 2008;586:4137-4153.**

635 **[30] Klugbauer N, Lacinova L, Flockerzi V, Hofmann F. Structure and functional**
636 **expression of a new member of the tetrodotoxin-sensitive voltage-activated**
637 **sodium channel family from human neuroendocrine cells. EMBO J**
638 **1995;14:1084-1090.**

639 **[31] Koenig J, Werdehausen R, Linley JE, Habib AM, Vernon J, Lolignier S,**
640 **Eijkelkamp N, Zhao J, Okorokov AL, Woods CG, Wood JN, Cox JJ. Regulation**
641 **of Nav1.7: A Conserved SCN9A Natural Antisense Transcript Expressed in**
642 **Dorsal Root Ganglia. PLoS One 2015;10:e0128830.**

643 **[32] Lawson SN. Phenotype and function of somatic primary afferent nociceptive**
644 **neurones with C-, Adelta- or Aalpha/beta-fibres. Exp Physiol 2002;87:239-244.**

645 **[33] Li QS, Cheng P, Favis R, Wickenden A, Romano G, Wang H. SCN9A Variants**
646 **May be Implicated in Neuropathic Pain Associated With Diabetic Peripheral**
647 **Neuropathy and Pain Severity. Clin J Pain 2015;31:976-982.**

648 **[34] Matsutomi T, Nakamoto C, Zheng T, Kakimura J, Ogata N. Multiple types of**
649 **Na(+) currents mediate action potential electrogenesis in small neurons of mouse**
650 **dorsal root ganglia. Pflugers Arch 2006;453:83-96.**

651 **[35] McDonnell A, Schulman B, Ali Z, Dib-Hajj SD, Brock F, Cobain S, Mainka T,**
652 **Vollert J, Tarabar S, Waxman SG. Inherited erythromelalgia due to mutations in**
653 **SCN9A: natural history, clinical phenotype and somatosensory profile. Brain**
654 **2016;139:1052-1065.**

655 **[36] Minett MS, Falk S, Santana-Varela S, Bogdanov YD, Nassar MA, Heegaard AM,**
656 **Wood JN. Pain without nociceptors? Nav1.7-independent pain mechanisms. Cell**
657 **Rep 2014;6:301-312.**

658 **[37] Minett MS, Nassar MA, Clark AK, Passmore G, Dickenson AH, Wang F,**
659 **Malcangio M, Wood JN. Distinct Nav1.7-dependent pain sensations require**
660 **different sets of sensory and sympathetic neurons. Nat Commun 2012;3:791.**

661 **[38] Minett MS, Pereira V, Sikandar S, Matsuyama A, Lolignier S, Kanellopoulos**
662 **AH, Mancini F, Iannetti GD, Bogdanov YD, Santana-Varela S, Millet Q,**
663 **Baskozos G, MacAllister R, Cox JJ, Zhao J, Wood JN. Endogenous opioids**

664 **contribute to insensitivity to pain in humans and mice lacking sodium channel**
665 **Nav1.7. Nat Commun 2015;6:8967.**

666 **[39] Moore JW, Joyner RW, Brill MH, Waxman SD, Najar-Joa M. Simulations of**
667 **conduction in uniform myelinated fibers. Relative sensitivity to changes in nodal**
668 **and internodal parameters. Biophys J 1978;21:147-160.**

669 **[40] Nassar MA, Stirling LC, Forlani G, Baker MD, Matthews EA, Dickenson AH,**
670 **Wood JN. Nociceptor-specific gene deletion reveals a major role for Nav1.7 (PN1)**
671 **in acute and inflammatory pain. Proc Natl Acad Sci U S A 2004;101:12706-**
672 **12711.**

673 **[41] Persson AK, Black JA, Gasser A, Cheng X, Fischer TZ, Waxman SG. Sodium-**
674 **calcium exchanger and multiple sodium channel isoforms in intra-epidermal**
675 **nerve terminals. Mol Pain 2010;6:84.**

676 **[42] Persson AK, Liu S, Faber CG, Merkies IS, Black JA, Waxman SG. Neuropathy-**
677 **associated Nav1.7 variant I228M impairs integrity of dorsal root ganglion neuron**
678 **axons. Ann Neurol 2013;73:140-145.**

679 **[43] Reeh PW. Sensory receptors in mammalian skin in an in vitro preparation.**
680 **Neurosci Lett 1986;66:141-146.**

681 **[44] Renganathan M, Cummins TR, Waxman SG. Contribution of Na(v)1.8 sodium**
682 **channels to action potential electrogenesis in DRG neurons. J Neurophysiol**
683 **2001;86:629-640.**

684 **[45] Rush AM, Dib-Hajj SD, Liu S, Cummins TR, Black JA, Waxman SG. A single**
685 **sodium channel mutation produces hyper- or hypoexcitability in different types**
686 **of neurons. Proc Natl Acad Sci U S A 2006;103:8245-8250.**

687 **[46] Sangameswaran L, Fish LM, Koch BD, Rabert DK, Delgado SG, Ilnicka M,**
688 **Jakeman LB, Novakovic S, Wong K, Sze P, Tzoumaka E, Stewart GR, Herman**
689 **RC, Chan H, Eglen RM, Hunter JC. A novel tetrodotoxin-sensitive, voltage-gated**
690 **sodium channel expressed in rat and human dorsal root ganglia. J Biol Chem**
691 **1997;272:14805-14809.**

692 **[47] Sauer SK, Schafer D, Kress M, Reeh PW. Stimulated prostaglandin E2 release**
693 **from rat skin, in vitro. Life Sci 1998;62:2045-2055.**

694 **[48] Schmelz M, Forster C, Schmidt R, Ringkamp M, Handwerker HO, Torebjork**
695 **HE. Delayed responses to electrical stimuli reflect C-fiber responsiveness in**
696 **human microneurography. Exp Brain Res 1995;104:331-336.**

697 **[49] Shields SD, Cheng X, Uceyler N, Sommer C, Dib-Hajj SD, Waxman SG. Sodium**
698 **channel Na(v)1.7 is essential for lowering heat pain threshold after burn injury. J**
699 **Neurosci 2012;32:10819-10832.**

700 **[50] Sleeper AA, Cummins TR, Dib-Hajj SD, Hormuzdiar W, Tyrrell L, Waxman**
701 **SG, Black JA. Changes in expression of two tetrodotoxin-resistant sodium**
702 **channels and their currents in dorsal root ganglion neurons after sciatic nerve**
703 **injury but not rhizotomy. J Neurosci 2000;20:7279-7289.**

704 **[51] Spitzer MJ, Reeh PW, Sauer SK. Mechanisms of potassium- and capsaicin-**
705 **induced axonal calcitonin gene-related peptide release: involvement of L- and T-**

706 type calcium channels and TRPV1 but not sodium channels. Neuroscience
707 2008;151:836-842.

708 [52] Sun W, Miao B, Wang XC, Duan JH, Wang WT, Kuang F, Xie RG, Xing JL, Xu
709 H, Song XJ, Luo C, Hu SJ. Reduced conduction failure of the main axon of
710 polymodal nociceptive C-fibres contributes to painful diabetic neuropathy in
711 rats. Brain 2012;135:359-375.

712 [53] Tigerholm J, Petersson ME, Obreja O, Lampert A, Carr R, Schmelz M, Fransen
713 E. Modeling activity-dependent changes of axonal spike conduction in primary
714 afferent C-nociceptors. J Neurophysiol 2014;111:1721-1735.

715 [54] Toledo-Aral JJ, Moss BL, He ZJ, Koszowski AG, Whisenand T, Levinson SR,
716 Wolf JJ, Silos-Santiago I, Halegoua S, Mandel G. Identification of PN1, a
717 predominant voltage-dependent sodium channel expressed principally in
718 peripheral neurons. Proc Natl Acad Sci U S A 1997;94:1527-1532.

719 [55] Waxman SG. Sodium channels, the electrogenisome and the electrogenistat:
720 lessons and questions from the clinic. J Physiol 2012;590:2601-2612.

721 [56] Weidner C, Schmelz M, Schmidt R, Hammarberg B, Orstavik K, Hilliges M,
722 Torebjork HE, Handwerker HO. Neural signal processing: the underestimated
723 contribution of peripheral human C-fibers. J Neurosci 2002;22:6704-6712.

724 [57] Weidner C, Schmidt R, Schmelz M, Hilliges M, Handwerker HO, Torebjork HE.
725 Time course of post-excitatory effects separates afferent human C fibre classes. J
726 Physiol 2000;527 Pt 1:185-191.

[58] Weiss J, Pyrski M, Jacobi E, Bufe B, Willnecker V, Schick B, Zizzari P, Gossage SJ, Greer CA, Leinders-Zufall T, Woods CG, Wood JN, Zufall F. Loss-of-function mutations in sodium channel Nav1.7 cause anosmia. Nature 2011;472:186-190.

[59] Xu W, Zhang J, Wang Y, Wang L, Wang X. Changes in the expression of voltage-gated sodium channels Nav1.3, Nav1.7, Nav1.8, and Nav1.9 in rat trigeminal ganglia following chronic constriction injury. Neuroreport 2016;27:929-934.

[60] Yang Y, Wang Y, Li S, Xu Z, Li H, Ma L, Fan J, Bu D, Liu B, Fan Z, Wu G, Jin J, Ding B, Zhu X, Shen Y. Mutations in SCN9A, encoding a sodium channel alpha subunit, in patients with primary erythermalgia. J Med Genet 2004;41:171-174.

[61] Yiangou Y, Facer P, Chessell IP, Bountra C, Chan C, Fertleman C, Smith V, Anand P. Voltage-gated ion channel Nav1.7 innervation in patients with idiopathic rectal hypersensitivity and paroxysmal extreme pain disorder (familial rectal pain). Neurosci Lett 2007;427:77-82.

[62] Zhang H, Dougherty PM. Enhanced excitability of primary sensory neurons and altered gene expression of neuronal ion channels in dorsal root ganglion in paclitaxel-induced peripheral neuropathy. Anesthesiology 2014;120:1463-1475.

[63] Zimmermann K, Leffler A, Babes A, Cendan CM, Carr RW, Kobayashi J, Nau C, Wood JN, Reeh PW. Sensory neuron sodium channel Nav1.8 is essential for pain at low temperatures. Nature 2007;447:855-858.

749

750